Journal of Alloys and Compounds 510 (2012) 60–65

Contents lists available at SciVerse ScienceDirect

Journal of Alloys and Compounds

journal homepage: www.elsevier.com/locate/jallcom

Correlating phase and microstructure development versus dielectric properties in La^{3+} and Er^{3+} co-doped $Bi_4Ti_3O_{12}$ ferroelectric ceramics

Valdeci Bosco dos Santos, Jean-Claude M'Peko*, Valmor Roberto Mastelaro

Instituto de Física de São Carlos (IFSC), Universidade de São Paulo (USP), C. Postal: 369, 13560-970 São Carlos – São Paulo, Brazil

ARTICLE INFO

Article history:
Received 9 November 2010
Received in revised form 11 August 2011
Accepted 12 August 2011
Available online 22 August 2011

Keywords:
Ceramics
Ferroelectrics
Sintering
Dielectric response
Microstructure

ABSTRACT

$Bi_{3.25}La_{0.75-x}Er_xTi_3O_{12}$ and $Bi_{3.25}La_{0.75}Ti_{3-x}Er_xO_{12-\delta}$ ceramics were prepared and studied in this work in terms of dopant-induced phase and microstructure development as well as dielectric response. The results show that introduction of Er^{3+} tends to reduce the materials' sintering temperature and average grain size. Moreover, it was noted that in these systems the substitution site of this dopant is controlled by valence state and ionic radii mismatch effects. In particular, even when a nominal substitution of Ti^{4+} is conceived, here it is found that Er^{3+} also incorporates at the $(Bi,La)^{3+}$ sites. These and other interesting concluding remarks from this work, including Er^{3+} tolerance, were possible only after comparing, especially, the X-ray diffraction results and the intrinsic ferroelectric characteristics extracted from the dielectric measurements.

1. Introduction

Bismuth titanate ($Bi_4Ti_3O_{12}$, BIT) is a ferroelectric material belonging to the Aurivillius family, and consists of $(Bi_2O_2)^{2+}$ sheets alternating with $(Bi_2Ti_3O_{10})^{2-}$ perovskite-like layers stacked along the crystallographic ***c*** direction [1,2]. Like other ferroelectric materials, BIT has a wide potential application in the electronic industry, which includes the manufacture of capacitors, memory devices as well as electrical and optical sensors. Doping ferroelectrics with foreign cations has been normally explored with the purpose of trying to improve given dielectric and/or optical properties from such materials, depending on the applications envisaged. This is the case of doping partially BIT with rare earths at the Bi^{3+} sites (homovalent-like substitution) and/or higher-valent cations at the Ti^{4+} sites (heterovalent-like substitution) [3–12]. Research on the La^{3+}-doped BIT ($Bi_{4-x}La_xTi_3O_{12}$, BLT100*x*) system has been particularly intense, from both experimental and simulation viewpoints [3,6,9,13], due to the finding that La^{3+} effectively improves the fatigue endurance of BLT with respect to BIT materials, especially for $x = 0.75$ [3]. Accordingly, La^{3+} incorporation in the BIT lattice reduces content of the oxygen vacancies that contribute to ferroelectric fatigue owing to a strong interaction with domain walls.

We recently conducted a comprehensive study of this BLT system in terms of La^{3+}-assisted sintering and microstructure development, La^{3+} tolerance, long-range structural and electrical properties [14]. With respect to foreign cation tolerance, for instance, it was shown by combining structural and electrical measurements that the solubility limit (x_L) of La^{3+} into BIT to form second phase-free BLT materials is located slightly above $x = 1.5$, in contrast to an earlier value of $x_L = 2.8$ from the literature [15,16]. The present work is intended to further advance this study by choosing to dope the BLT system (starting from the BLT075 composition) with Er^{3+} at either the $(Bi,La)^{3+}$ or the Ti^{4+} sites, with the purpose of exploring the correlation between important characteristics such as (micro)structure development, Er^{3+} solubility and resulting ferroelectric properties. To the best of our knowledge, comprehensive works exploring the effect of Er^{3+} on these characteristics in BIT-based ceramic materials are scarce in the literature.

2. Experimental procedures

Er^{3+}-doped $Bi_{3.25}La_{0.75}Ti_3O_{12}$ (BLT075) ceramics were prepared via the conventional solid-state reaction method. Nominally, the systems considered to be produced were $Bi_{3.25}La_{0.75-x}Er_xTi_3O_{12}$ (BLExT) and $Bi_{3.25}La_{0.75}Ti_{3-x}Er_xO_{12-\delta}$ (BLTEx), with $x = 0.02$, 0.04 and 0.06, hereafter denoted as BLE02T, BLE04T and BLE06T, on the one hand, and BLTE02, BLTE04 and BLTE06, on the other hand. Starting from high-purity raw materials (from Alfa Aesar): Bi_2O_3 (99.5%), La_2O_3 (99.999%), Er_2O_3 (99.9%), and TiO_2 (99.9%), the powders were weighted in the appropriate stoichiometric amounts, mixed and ball-milled for 36 h in polyethylene vases while dispersed in isopropyl alcohol. The mixed powders were calcined at 860 °C for 6 h, and then ball-milled again for 12 h in the aforementioned plastic recipients with isopropyl alcohol. After drying, these powders were pressed into disk-shaped samples and then sintered at 1115 °C for 2 h, after various heat-treatment tests. Following the results on optimal sintering conditions of the BLT materials previously reported in Ref. [14], the BLT075 samples were also sintered at 1195 °C for 2 h (hereafter denoted as BLT075*). The density of these ceramics was measured by the Archimedes method. Moreover, the crystalline structures of these materials

* Corresponding author. Tel.: +55 16 33739828; fax: +55 16 33739824.
E-mail address: peko@if.sc.usp.br (J.-C. M'Peko).

0925-8388/$ – see front matter © 2011 Elsevier B.V. All rights reserved.
doi:10.1016/j.jallcom.2011.08.062

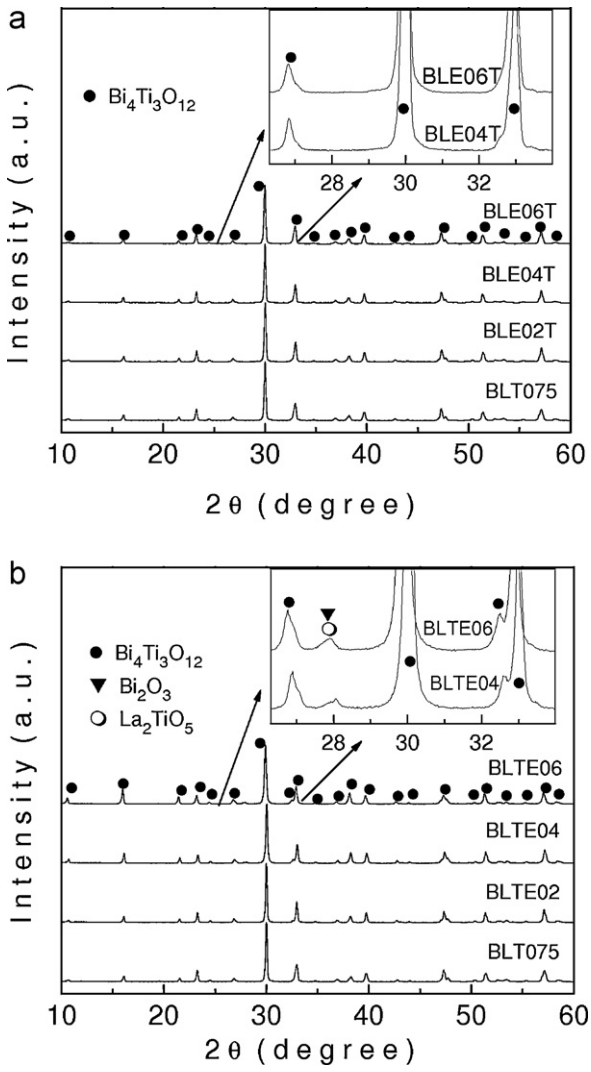

Fig. 1. XRD patterns of the calcined (a) $Bi_{3.25}La_{0.75-x}Er_xTi_3O_{12}$ (BLExT) and (b) $Bi_{3.25}La_{0.75}Ti_{3-x}Er_xO_{12-\delta}$ (BLTEx) powders. Both graphs include the XRD results from the calcined BLT075 powder. All these patterns show peaks corresponding to a phase isostructural with $Bi_4Ti_3O_{12}$ (JCPDS: 35-0795). For BLTE04 and BLTE06, additional low-intensity phases isostructural with Bi_2O_3 (JCPDS: 74-1375) and/or La_2TiO_5 (JCPDS: 75-2394) were identified.

were characterized by X-ray diffraction (XRD) using a Rigaku-Rotaflex RU-200B diffractometer (50 kV × 100 mA) with Cu $K\alpha_1$ ($\lambda = 1.5405$ Å). Also, scanning electron microscopy (SEM) observations of the ceramics were performed using a Zeiss DSM960 microscope. The latter was fitted with fully automated equipment for quantitative energy-dispersive X-ray spectroscopy (EDS) analysis. Electrical measurements of the ceramic samples were conducted in a Solartron SI 1260 impedance analyzer at selected frequencies in the 1 Hz–1 MHz range, over a wide temperature range from 25 to 600 °C, and using Pt electrodes. From these measurements, parameters such as dielectric permittivity and Curie temperature were evaluated.

3. Results and discussion

Fig. 1 shows the room-temperature XRD patterns of the BLT075, BLExT and BLTEx powders calcined at 860 °C for 6 h. For the undoped BLT075 powder, a single BIT-like phase was detected. The same result applies for the BLExT system (Er^{3+} nominally introduced at the La^{3+} sites), as seen in Fig. 1(a). Meanwhile, the XRD spectra corresponding to the BLTEx system (Er^{3+} nominally incorporated at the Ti^{4+} sites) were free of secondary phase for $x = 0.02$, but showed additional Bi_2O_3 and/or La_2TiO_5 (L2T1) phase for $x \geq 0.04$, Fig. 1(b). An important observation in the latter case

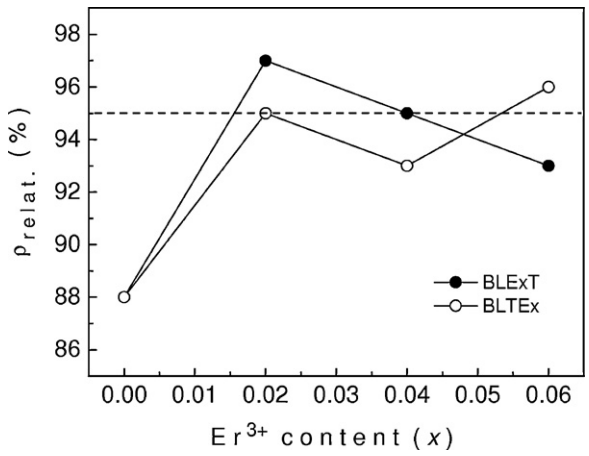

Fig. 2. Dependence of the relative density (ρ_{relat}) of the $Bi_{3.25}La_{0.75-x}Er_xTi_3O_{12}$ (BLExT) and $Bi_{3.25}La_{0.75}Ti_{3-x}Er_xO_{12-\delta}$ (BLTEx) ceramic samples (sintered at 1115 °C for 2 h) upon variation of Er^{3+} content. The horizontal dashed line is merely a reference indicating the density value of the BLT075* sample sintered at 1195 °C for 2 h.

(BLTEx system) is that, after calcination, the powders resulted in slightly to significantly agglomerated, with increasing Er^{3+} content, while changing their coloration from light-yellowish brown to dark-yellowish brown. These effects are here considered to involve the melting of Bi_2O_3 (one of the two possible secondary phases detected for $x > 0.02$ in the XRD patterns presented in Fig. 1(b)) expected to occur at a temperature as low as 820 °C [17]. The melting point of L2T1 is located at a much higher temperature, close to 1700 °C [18]. In Fig. 1(b), in fact, the XRD peak intensity corresponding to the Bi_2O_3 phase, presumed to likely be the dominant phase (compared to L2T1, if any) is seen to increase with rising Er^{3+} concentration.

With respect to the thermal conditions to achieve the materials' optimal sintering and densification, it is important to remember, from the preceding work [14], that BLT075 samples were heat-treated at 1195 °C for 2 h to obtain high-density bodies (95% of its own XRD-derived theoretical density, TD = 7.688 g/cm^3). This also applies to the BLT075* ceramic samples prepared here. In contrast, any attempt to produce the BLExT and BLTEx ceramics at these sintering conditions, or at even higher temperatures (up to 1280 °C for 2 h), only led, in both systems, to second phase formation (consisting of Er_2TiO_5, E2T1, and/or L2T1, according to XRD measurements) and poor densities towards the highest sintering temperatures tested [19]. Conducting that systematic study allowed to consider the conditions of 1115 °C and 2 h as better ones for producing relatively high- to high-quality ceramics. Fig. 2 illustrates the behavior of the materials' relative density (ρ_{relat}) with increasing Er^{3+} content. Densities corresponding to the doped materials reached values ranging from 93 to 97% (of BLT075 TD), remaining higher than the value of 88% TD obtained for the undoped BLT075 ceramics. Full understanding of the density behaviors observed in this figure required, however, the analysis of other results from this work, as will be discussed later. In any case, Er^{3+} appears to reduce the energy barrier associated with cation diffusion during sintering and densification of these materials. That is, as the optimal sintering of high-density undoped BLT075 samples occurs around 1195 °C (BLT075* ceramics, averaging about 95% TD) [14], it can be thus stated that Er^{3+} actually reduces the sintering temperature of this system. Recently, a study on V^{5+}-doped BIT ceramics (with V^{5+} substituting for Ti^{4+}) showed an analogous dopant-induced sintering trend [7].

Fig. 3 shows the room-temperature XRD patterns collected from the BLT075*, BLExT and BLTEx ceramic samples after

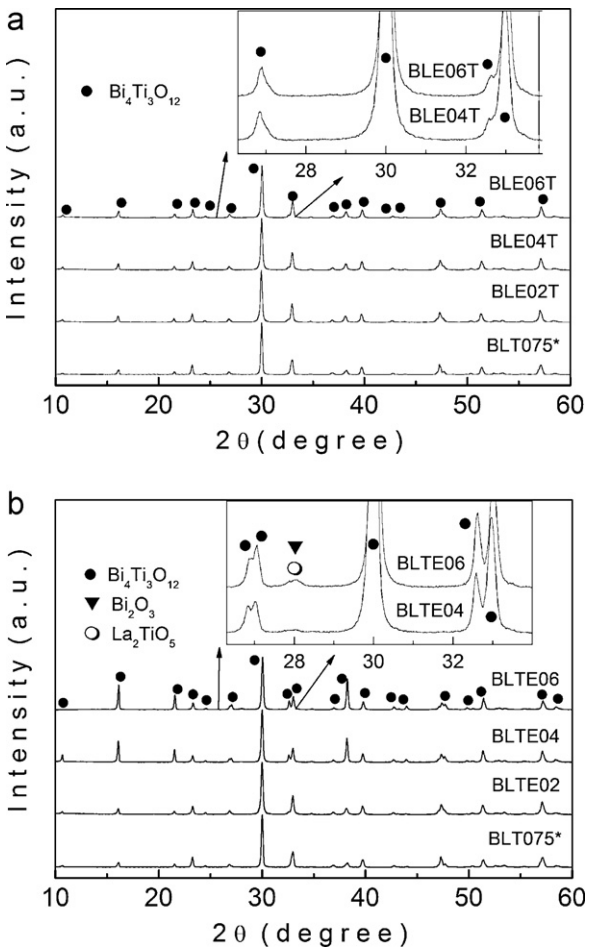

Fig. 3. XRD patterns of the sintered (a) $Bi_{3.25}La_{0.75-x}Er_xTi_3O_{12}$ (BLExT) and (b) $Bi_{3.25}La_{0.75}Ti_{3-x}Er_xO_{12-\delta}$ (BLTEx) ceramic samples. For reference, both graphs include the results from the high-density BLT075* ceramic sample. All these patterns show peaks corresponding to a phase isostructural with $Bi_4Ti_3O_{12}$ (JCPDS: 35-0795). For BLTE04 and BLTE06, again, additional low-intensity phases isostructural with Bi_2O_3 (JCPDS: 74-1375) and/or La_2TiO_5 (JCPDS: 75-2394) were identified.

sintering at 1195 °C for 2 h, for the undoped material, and 1115 °C for 2 h, for the Er^{3+}-doped BLT075 materials. These XRD spectra are similar to those shown in Fig. 1, with persistence of traces from Bi_2O_3 (seemingly major) and L2T1 (if any) phases for the BLTEx ceramics, for $x \geq 0.04$ (Fig. 3(b)). These results are apparently indicative that, while Er^{3+} is totally soluble in the BLT075 system when being nominally incorporated at the La^{3+} sites (at least up to $x = 0.06$), this does not seem to be the case when trying to introduce Er^{3+} at the Ti^{4+} sites, as a XRD-associated solubility limit would be proposed to occur for $x = 0.02$. Considering that the secondary phase involves Bi_2O_3 and/or L2T1, the proposition of a partial incorporation of Er^{3+} also at the $(Bi,La)^{3+}$ sites for $x > 0.02$ is hereby straightforward for the BLExT system. Indeed, this observation should apply as well for $x = 0.02$ (BLTE02 sample), as its calcined powder also resulted slightly agglomerated and with a light-yellowish brown color (ascribed to Bi_2O_3 melting), different from the original, comparatively deagglomerated and white-like BLT075 calcined powder. This is comprehensible if considering, from the valence state viewpoint, that the substitution of $(Bi,La)^{3+}$ by Er^{3+} should normally be first expected with respect to the substitution of Ti^{4+}.

In terms of preference, the above incorporation trend of Er^{3+} at the $(Bi,La)^{3+}$ sites is also predictable from the viewpoint of stress energy minimization in the BIT structure during doping, by comparing the ionic radii (IR) of the foreign versus host cations. For Er^{3+} introduction at the $(Bi,La)^{3+}$ sites, with a twelve-coordination number, it applies that $IR(Er^{3+}) = 1.22$ Å, while $IR(Bi^{3+}) = 1.40$ Å and $IR(La^{3+}) = 1.36$ Å [20], implying that $\Delta IR(Bi\text{-}Er) = 0.18$ Å and $\Delta IR(La\text{-}Er) = 0.14$ Å. This substitution event is expected to produce stress effects significantly lower than incorporation of Er^{3+} at the Ti^{4+} sites, with a six-coordination number: $IR(Er^{3+}) = 0.89$ Å and $IR(Ti^{4+}) = 0.61$ Å [20], implying that $\Delta IR(Er\text{-}Ti) = 0.28$ Å. From this analysis and the above observations (including coloration trend), it is possible to conclude that, even when nominally prepared so as to substitute Ti^{4+}, Er^{3+} cations also incorporate at the $(Bi,La)^{3+}$ sites for all the BLTEx compositions. Regarding the BLExT system, substitution of La^{3+} by Er^{3+} remains in total accordance with the predictable result from both valence state and energy stress viewpoints, the final materials resulting apparently free of second phase, at least within the detection limit of the XRD technique (about 5 wt%).

Fig. 4 illustrates the SEM micrographs from the dense BLT075*, BLE02T, BLE06T, BLTE02 and BLTE06 ceramic samples. BIT ceramics are known to normally show plate-like grains. According to Ref. [14], when introduced into the BIT system, La^{3+} has the trend of gradually transforming these grains to a spherical form, as well as promoting a grain growth inhibition process. In the present work, we chose to characterize the microstructure morphology of these ceramic materials by estimating the average aspect ratio $R = a/b$ of the grains [21] (see indication of a and b exemplified in Fig. 4(a)). Accordingly, $R > 1$ and $R \cong 1$ represent the formation trend of, respectively, plate-like and spherical-like grains. For BLT075*, on the one hand, the estimated value of aspect ratio was $R \cong 2.8$. For the doped materials, on the other hand, R varied slightly but sensitively from about 1.5 to 2.1, for the BLExT system, and significantly from about 2.3 to 4.2, for the BLTEx one, while varying x from 0.02 to 0.06. From these results and a direct comparison between the images illustrated in Fig. 4, it is concluded that the presence of Er^{3+} has the effect of favoring a decrease of the aspect ratio of the plate-like grains in these materials, besides causing an evident decrease in the materials' final average grain size, that is, except for BLTE06 (Fig. 4(e)) when compared with BLT075 (Fig. 4(a)), the justification being given below. Together with the fact that R from the BLTEx materials is greater than that from the BLExT ones, the substantial increase of R with rising Er^{3+} in this BLTEx system should arise from the development of liquid phase-assisted sintering, most likely involving, as proposed above, the low-temperature melting of Bi_2O_3. As well known from the literature on sintering of materials, presence of a liquid phase generally promotes grain growth, by the occurrence of cations dissolution, mass transport and re-precipitation processes [22,23].

Fig. 5 illustrates the temperature dependence of dielectric permittivity (ε) measured in these BLT075*, BLExT and BLTEx ceramic materials at 1 MHz. As expected for ferroelectrics, the curves show dielectric peaks that correspond to the ferro- to para-electric phase transition occurring at the Curie temperature (T_c), followed by a monotonous decrease of permittivity above T_c, in accordance with Curie–Weiss law prediction. For all these materials, the behaviors of T_c and maximum permittivity, $\varepsilon_m \equiv \varepsilon(T_c)$ upon variation of Er^{3+} are shown in Fig. 6. The decrease of T_c and ε_m in the doped materials, with respect to undoped BLT075*, may be accounted for by considering that Er^{3+} should reduce the ferroelectricity strength of such materials. Getting further insights into the characteristics of these materials requires, however, a close interpretation of the T_c and ε_m variations between samples within each BLExT or BLTEx system. According to the XRD results shown in Fig. 3(a), for instance, there was presumably no solubility limit of Er^{3+} into BLT075, when this foreign cation was incorporated at the La^{3+} sites, at least over the composition range studied here (up to $x = 0.06$). However, according to Fig. 6(a), T_c from these BLExT ceramics decreases from $x = 0$ to $x = 0.02$, but remains thereafter constant

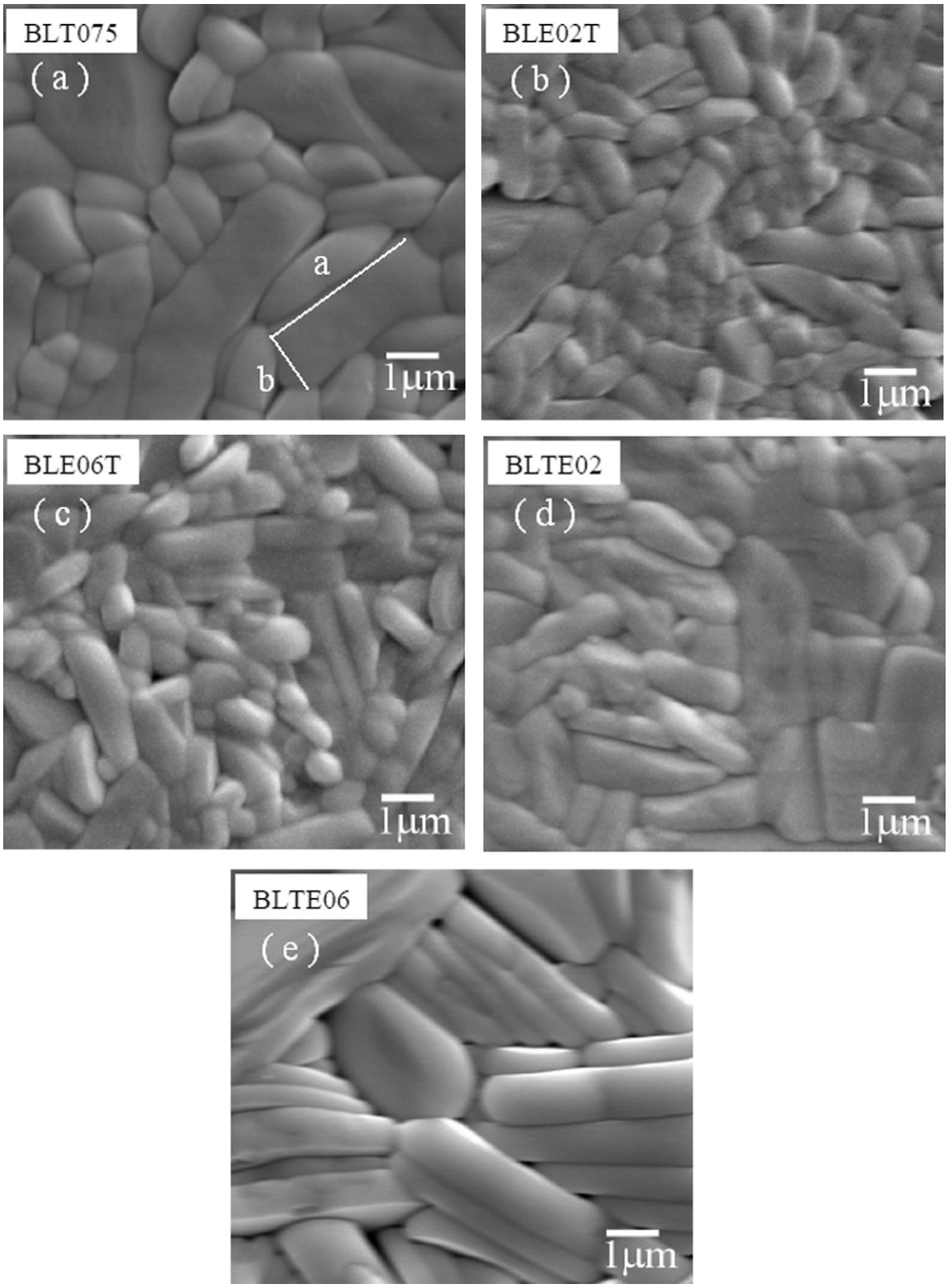

Fig. 4. SEM micrographs of the sintered (a) BLT075*, (b) BLE02T, (c) BLE06T, (d) BLET02 and (e) BLET06 ceramic samples. The grain morphology-associated *a* and *b* lengths, indicated in (a), were used to estimate the aspect ratio $R = a/b$ for each sample (see text).

(for $x \geq 0.02$). As T_c is an intrinsic property of ferroelectric materials, the direct conclusion is the existence of a tolerance limit of Er^{3+} when substituting La^{3+} into BLT075 up to $x = 0.02$, that is, irrespective of the non detection in this (BLExT) system of second phase formation by XRD, a fact attributable to the equipment's sensitivity limitation.

At this stage, we chose to proceed with the analysis of the results from the EDS measurements performed in this work. Table 1 shows

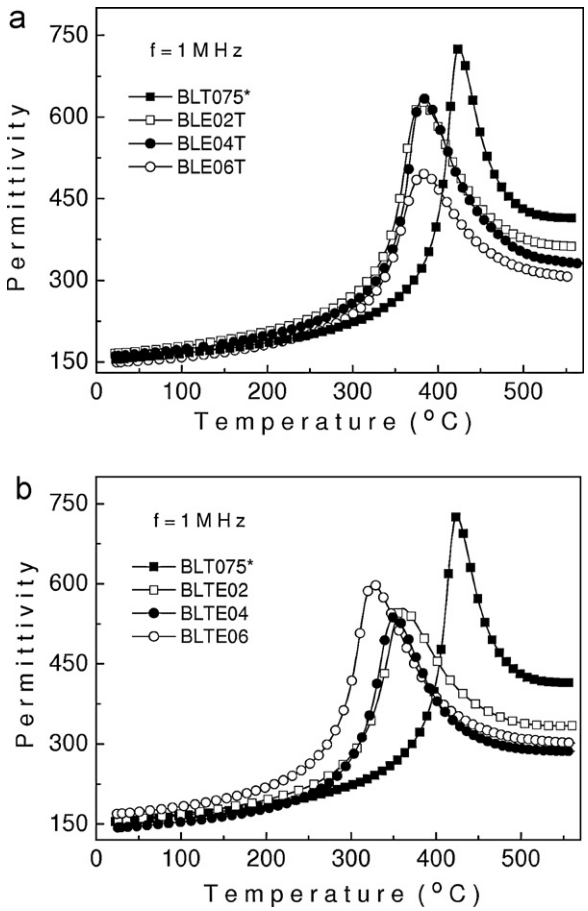

Fig. 5. Temperature dependence of permittivity measured at 1 MHz for the sintered (a) $Bi_{3.25}La_{0.75-x}Er_xTi_3O_{12}$ (BLExT) and (b) $Bi_{3.25}La_{0.75}Ti_{3-x}Er_xO_{12-\delta}$ (BLTEx) ceramic samples. For reference, both graphs include the results from the high-density BLT075* ceramic sample.

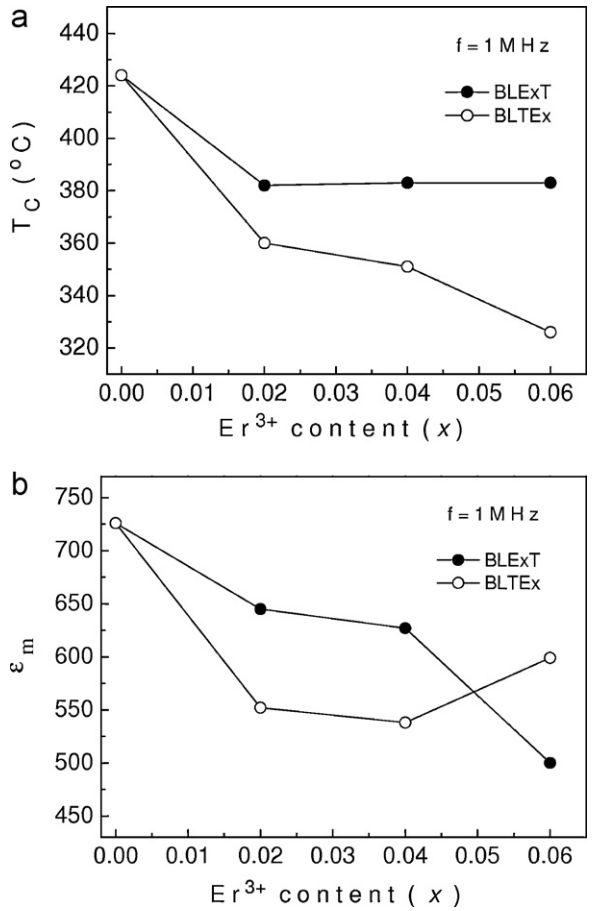

Fig. 6. Dependence of the (a) Curie temperature (T_c) and (b) maximum permittivity (ε_m) of the sintered $Bi_{3.25}La_{0.75-x}Er_xTi_3O_{12}$ (BLExT) and $Bi_{3.25}La_{0.75}Ti_{3-x}Er_xO_{12-\delta}$ (BLTEx) ceramic samples upon variation of Er^{3+} content. In both cases, the data for $x = 0$ correspond to BLT075*.

the nominal and experimental relative values of the grain-bulk chemical elements of direct concern, as detected in the Er^{3+}-doped BLT075 materials. For BLExT, values of the La/Er ratio suggest, within the (relatively low) margin of error of the measurements and compared with the behavior that would be expected from the nominal composition, almost unchanged concentrations of Er^{3+} and La^{3+} in these materials for $x \geq 0.02$, in good agreement with the information of an unchanged value of T_C, as extracted from the dielectric study. In practice, during sintering, the excess of Er^{3+} should most likely segregate at the grain-boundary interfaces. The results presented earlier are truly instructive, provided that they show how simple measurements, like the electrical ones conducted in this work, may result in even higher sensitivity than XRD measurements for detecting solubility limit and second phase formation in ferroelectric-like materials. Indeed, this observation also applies to the BLTEx ceramic materials studied in this work. That is, looking again at Fig. 6(a), the values of T_c corresponding to these materials incessantly decrease with rising Er^{3+} content, contrasting with a presumed solubility limit of Er^{3+} occurring for $x \cong 0.02$, according to the XRD results (Fig. 3(b)). The above T_c behavior instead suggests that, up to at least $x = 0.06$, Er^{3+} continuously incorporates into the BLTEx lattice. This observation agrees well with the EDS results presented in Table 1, showing a continuous variation of the Ti/Er ratio in these materials. Accordingly, it is reasonable to conclude that, even when conceived to incorporate at the Ti^{4+} sites, Er^{3+} also substitutes $(Bi,La)^{3+}$, certainly because of valence state similarity (3+) and lower ionic radii mismatch: ΔIR (Bi-Er) = 0.18 Å and ΔIR(La-Er) = 0.14 Å, while ΔIR(Er-Ti) = 0.28 Å. This fact should account for the detection of second phase formation in this system (Fig. 3(b)), not directly linked here, however, to a given solubility limit.

These findings help to further advance analysis and discussion, in a correlative fashion, of the results presented in Figs. 2, 4 and 6(b). Starting from the oxides mixture formulation (OMF) of, for instance, BLExT: $OMF \equiv 1.625Bi_2O_3 + (0.375-x/2)La_2O_3 + (x/2)Er_2O_3 + 3TiO_2$, the compositional formula after sintering (CFAS) of the corresponding samples should be proposed as follows. For $x = 0.02$, $CFAS \equiv Bi_{3.25}La_{0.73}Er_{0.02}Ti_3O_{12}$, this composition representing that of maximum solubility ($x \equiv x_L$) of Er^{3+} into this system. For $x = 0.06$, for example, stoichiometric calculations based on the above fact allow to estimate that $CFAS \equiv 0.945Bi_{3.25}La_{0.73}Er_{0.02}Ti_3O_{12} + \Omega(Bi,Er)$, where $\Omega(Bi,Er) \equiv 0.0891Bi_2O_3 + 0.0206Er_2O_3$ represents the excess of Bi^{3+} and Er^{3+} cations (given in terms of their corresponding oxides). In the case of a full mixture tolerance between these oxides

Table 1
Nominal versus experimental relative values of the grain-bulk chemical elements of concern for the $Bi_{3.25}La_{0.75-x}Er_xTi_3O_{12}$ (BLExT) and $Bi_{3.25}La_{0.75}Ti_{3-x}Er_xO_{12-\delta}$ (BLTEx) ceramic samples (La/Er and Ti/Er ratios, respectively), as extracted from repeated EDS measurements.

x	La/Er in BLExT		Ti/Er in BLTEx	
	Nom.	Exp. (±7)	Nom.	Exp. (±9)
0.02	36.5	42	149	141
0.04	17.8	31	74	80
0.06	11.5	36	49	55

during sintering, the above cation excess would involve the formation of two phases, *i.e.*, $\Omega(Bi,Er) \equiv 0.0411ErBiO_3 + 0.0685Bi_2O_3$. For the BLTEx samples, simultaneous insertion of Er^{3+} at both Ti^{4+} and $(Bi,La)^{3+}$ sites renders difficult to accurately predict their compositional formula after sintering. Nevertheless, over the composition range of total solubility, the corresponding oxides mixture, $1.625Bi_2O_3 + 0.375La_2O_3 + (3-x)TiO_2 + (x/2)Er_2O_3$, should lead to the synthesis of materials with the $(Bi,La,Er)_4(Ti,Er)_3O_{12-\delta} + \Omega(Bi,La)$ formula, with the possibility of L2T1 (second phase) formation being accordingly discarded (stoichiometry viewpoint).

In terms of final properties, different contributing effects may be anticipated from the aforementioned phase development facts. First, the presence of the secondary phases, with normally spherical-like grains, embedded into a BIT-based matrix, with typically plate-like grains, is expected to cause a decrease in the materials' final density (ρ_{relat}), as seen in Fig. 2 for the BLExT samples, for $x \geq 0.02$, and the BLTEx ones, from $x = 0.02$ to 0.04. Second, the excess of Bi_2O_3 should account for the increase in aspect ratio (R) observed in all these samples with increasing Er^{3+} content (Fig. 4), due to the development of a Bi_2O_3-associated liquid phase-assisted sintering mechanism [22,23]. Third, provided their non ferroelectric nature, these secondary phases are also supposed to lead to a decrease in the materials' permittivity (ε_m) with rising Er^{3+} content (Fig. 6(b)), that is, besides recognizing that such a result should also involve, of course, the deleterious effect from a decrease in the materials' density (ρ_{relat}), Fig. 2, as found elsewhere [24,25]. For the BLTEx system, in fact, the behavior of maximum permittivity (ε_m) for $x \geq 0.02$ (Fig. 6(b)) shows to nearly follow the behavior of the materials' density (Fig. 2). In particular, the development of a Bi_2O_3 liquid phase-assisted sintering, as suggested above, should in this case account for the observation of higher density and, hence, permittivity values (Figs. 2 and 6(b), respectively) even for $x = 0.06$. For the BLExT system, the effect of the materials' density improvement associated with liquid phase-assisted sintering, as could be expected [22], was not observed here (Fig. 2), probably due to the quite low quantity of the Bi_2O_3 secondary phase involved, as proposed and discussed above.

3.1. Conclusions

$Bi_{3.25}La_{0.75-x}Er_xTi_3O_{12}$ and $Bi_{3.25}La_{0.75}Ti_{3-x}Er_xO_{12-\delta}$ ceramics were prepared and studied in this work. It was noted that Er^{3+} tends to reduce both materials' sintering temperature and average grain size. By comparing X-ray diffraction, SEM, EDS and dielectric results, the other important conclusions arising from this work can be summarized as follows: (a) the incorporation site of Er^{3+} in these ceramic materials is regulated by valence state and ionic radii-associated stress energy effects; (b) Er^{3+} shows a tolerance limit of about $x = 0.02$ when introduced into the system so as to nominally substitute La^{3+}; (c) when introduced in the system so as to substitute Ti^{4+}, Er^{3+} also incorporates at the $(Bi,La)^{3+}$ sites, a fact that promotes second phase formation not directly linked to a given solubility limit; and (d) the strength of the dielectric properties of these materials shows to include effects from both substitution site and materials density.

Acknowledgments

The authors gratefully acknowledge financial support from FAPESP and CNPq, two Brazilian research-funding agencies, and the anonymous reviewers for their helpful comments and suggestions.

References

[1] J.M. Herbert, Ferroelectric Transducers and Sensors, Gordon and Breach Science Publishers, New York, 1982.
[2] Y. Xu, Ferroelectric Materials and their Applications, Elsevier Science Publishers, 1991.
[3] B.H. Park, B.S. Kang, S.D. Bu, T.W. Noh, J. Lee, W. Jo, Nature 401 (1999) 682–684.
[4] T. Kojima, T. Sakai, T. Watanabe, H. Funakubo, K. Saito, M. Osada, Appl. Phys. Lett. 80 (2002) 2746–2748.
[5] M. Chen, Z.L. Liu, Y. Wang, C.C. Wang, X.S. Yang, K.L. Yao, Solid State Commun. 130 (2004) 735–739.
[6] C.H. Song, W. Li, J. Ma, J. Gu, Y.Y. Yao, Y. Feng, X.M. Lu, J.S. Zhu, Y.N. Wang, W.L.H. Chan, C.L. Choy, Solid State Commun. 129 (2004) 775–780.
[7] Q.-Y. Tang, Y.-M. Kan, Y.-G. Li, G.-J. Zhang, P.-L. Wang, Scripta Mater. 54 (2006) 2075–2080.
[8] P.Y. Goh, K.A. Razak, S. Sreekantan, J. Alloys Compd. 475 (2009) 758–761.
[9] W. Wang, H. Ke, J. Rao, J. Feng, M. Feng, D. Jia, Y. Zhou, J. Alloys Compd. 509 (2011) 4722–4725.
[10] H. Zhou, G.H. Wu, N. Qin, D.H. Baow, J. Am. Ceram. Soc. 93 (2010) 2109–2112.
[11] F. Gao, G.J. Ding, H. Zhou, G.H. Wu, N. Qin, D.H. Bao, J. Appl. Phys. 109 (2011) 043106.
[12] G. Ding, F. Gao, G. Wu, D. Bao, J. Appl. Phys. 109 (2011) 123101.
[13] S.H. Shah, P.D. Bristowe, J. Phys.: Condens. Matter 23 (2011) 155902.
[14] V.B. Santos, J.-C. M'Peko, M. Mir, V.R. Mastelaro, A.C. Hernandes, J. Eur. Ceram. Soc. 29 (2009) 751–756.
[15] R.W. Wolfe, R.E. Newnham, J. Electrochem. Soc. 116 (1969) 832–835.
[16] R.A. Armstrong, R.E. Newnham, Mater. Res. Bull. 7 (1972) 1025–1034.
[17] G.V. Samsonov, The Oxide Handbook, IFI/Plenum, New York, 1973.
[18] S.D. Skapin, D. Kolar, D. Suvorov, J. Eur. Ceram. Soc. 20 (2000) 1179–1185.
[19] V.B. Santos, Ph.D. These, Materials Science and Engineering Program, Institute of Physics at São Carlos, University of São Paulo, 2009.
[20] R.D. Shannon, C.T. Prewitt, Acta Cryst. B 25 (1969) 925–946.
[21] J.S. Reed, Principles of Ceramics Processing, 2nd ed., John Wiley & Sons, New York, 1995.
[22] T.-F. Lin, C.-T. Hu, I.-N. Lin, J. Am. Ceram. Soc. 73 (1990) 531–536.
[23] H.-Y. Lee, R. Freer, J. Appl. Phys. 81 (1997) 376–382.
[24] D.A. Payne, L.E. Cross, in: R.M. Fulrath, J.A. Pask (Eds.), Ceramic Microstructures '76, Westview Press, Boulder, 1976, p. 584.
[25] C.Y. Ng, K.A. Razak, J. Alloys Compd. 509 (2011) 942–947.